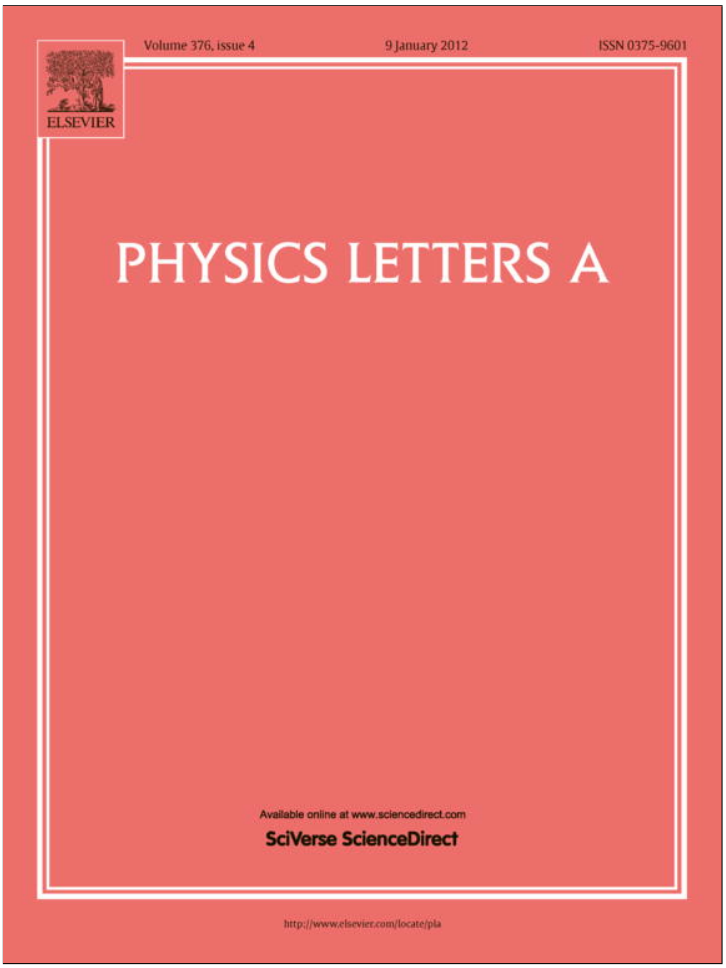

Physics Letters A 376 (2012) 442–446

Contents lists available at SciVerse ScienceDirect

Physics Letters A

www.elsevier.com/locate/pla

Hopf bifurcation control via a dynamic state-feedback control

Le Hoa Nguyen [a,1], Keum-Shik Hong [b,*]

[a] School of Mechanical Engineering, Pusan National University, 30 Jangjeon-dong, Gumjeong-gu, Busan 609-735, Republic of Korea
[b] Department of Cogno-Mechatronics Engineering and School of Mechanical Engineering, Pusan National University, 30 Jangjeon-dong, Gumjeong-gu, Busan 609-735, Republic of Korea

ARTICLE INFO

Article history:
Received 29 August 2011
Received in revised form 26 November 2011
Accepted 27 November 2011
Available online 30 November 2011
Communicated by C.R. Doering

Keywords:
Bifurcation control
Hopf bifurcation
Dynamic state-feedback control

ABSTRACT

To relocate two Hopf bifurcation points, simultaneously, to any desired locations in n-dimensional nonlinear systems, a novel dynamic state-feedback control law is proposed. Analytical schemes to determine the control gains according to the conditions for the emergence of Hopf bifurcation are derived. To verify the effectiveness of the proposed control law, numerical examples are provided.

1. Introduction

Bifurcation control has attracted many researchers due to its promising potential applications in various areas: the prevention of voltage collapse in electric power systems [1,2], the stabilization of rotating stall and surge in axial flow compressors [3,4], the regulation of human heart rhythms and neuronal activity behavior [5–7], the elimination of seizing activities in human cerebral cortex [8], and so on. In general, bifurcation control deals with designing a control law that is capable of modifying the bifurcation characteristics such as relocating the onset of an inherent bifurcation, modifying the stability and amplitudes of a bifurcated solution or branch, creating a new bifurcation at a desired parameter value, etc. [9]. Various bifurcation control approaches have been proposed in the literature [10–16]. Particularly, for the problem of relocating an inherent Hopf bifurcation, Wang and Abed [11] proposed a dynamic state-feedback control law incorporating a washout filter. Since then, the washout filter-aided dynamic feedback control has been widely applied in controlling the Hopf bifurcation in various bifurcating nonlinear systems [6,7,17–20]. Later, a static state feedback control with polynomial functions was proposed by Yu and Chen [13]. However, these methods cannot be applied to the systems with two Hopf bifurcations, since the relocation of one Hopf bifurcation point affects the location of the other [7,17]. Therefore, in general, it is needed to design a control law that can relocate both points to their individual desired positions. To the best of the authors' knowledge, such Hopf bifurcation control problem has not been investigated yet.

In this Letter, a novel dynamic state-feedback control law is derived for controlling the Hopf bifurcations in an n-dimensional nonlinear system. The proposed control law is able not only to relocate two different Hopf bifurcation points to any designated parameter values simultaneously but also to preserve all the equilibrium points of the system. According to the conditions [21] for the emergence of Hopf bifurcations without using eigenvalues, the procedure for deducing the control gains is derived analytically. The effectiveness of the proposed control law is verified through numerical examples. Throughout the Letter, R and R^n denote the real number set and the n-dimensional Euclidean space, respectively. I_n presents the identity matrix of dimension n, and $0_{n\times m}$ denotes the $n \times m$ null matrix.

The rest of this Letter is organized as follows. In Section 2, the conditions for the emergence of Hopf bifurcations are reviewed. In Section 3, a novel dynamic state-feedback control law for controlling Hopf bifurcation is proposed. The procedure to deduce the control gains is also derived in this section. In Section 4, we provide numerical examples to verify the effectiveness of the proposed bifurcation control method. Finally, conclusions are given in Section 5.

2. Conditions for the emergence of Hopf bifurcations

Consider the following n-dimensional nonlinear system.

$$\dot{x} = f(x, \mu),$$
$$f : R^{n+1} \to R^n, \quad x \in R^n, \ \mu \in R, \tag{1}$$

* Corresponding author. Tel.: +82 51 510 2454; fax: +82 51 514 0685.
E-mail addresses: nglehoa@pusan.ac.kr (L.H. Nguyen), kshong@pusan.ac.kr (K.-S. Hong).
[1] Tel.: +82 51 510 2973; fax: +82 51 514 0685.

0375-9601/$ – see front matter
doi:10.1016/j.physleta.2011.11.057

where x is the state vector, μ is the bifurcation parameter, and the vector field $f(x,\mu)$ is smooth in x and μ. Suppose that the system (1) has an equilibrium point at $x = x^e$, for some $\mu = \mu^e$, i.e., $f(x^e,\mu^e) = 0$. Let $J(x^e,\mu^e) = \partial f(x,\mu)/\partial x|_{x=x^e,\,\mu=\mu^e}$ be the Jacobian matrix evaluated at the equilibrium point. Assume that the following two conditions are satisfied:

(i) Eigenvalue crossing condition: The Jacobian matrix $J(x^e,\mu^e)$ has a pair of pure imaginary eigenvalues $\lambda(\mu^e) = \pm j\omega$, and the other eigenvalues have negative real parts.
(ii) Transversality condition: The eigenvalues $\lambda(\mu^e)$ cross the imaginary axis at some nonzero speed, i.e.,

$$\left.\frac{d(\operatorname{Re}\lambda(\mu))}{d\mu}\right|_{\mu=\mu^e} \neq 0. \tag{2}$$

Then, the system (1) undergoes a Hopf bifurcation at $\mu = \mu^e$. The conditions (i) and (ii) provide the traditional criteria for detecting the existence of Hopf bifurcations, which is stated in terms of the properties of eigenvalues. In order to create a Hopf bifurcation at a desired parameter value by using a control signal, one expects to obtain analytical expressions of all the eigenvalues of the Jacobian matrix of the closed-loop system as functions of control gains. However, for a high-dimensional system, such analytical expressions are very difficult to obtain or even impossible. To avoid a direct solving of all the eigenvalues, Liu [21] derived an equivalent criterion for the Hopf bifurcation, which is stated in terms of the coefficients of the characteristic polynomial instead of expressions for the eigenvalues, as stated below.

Let the characteristic polynomial of the Jacobian matrix $J(x^e,\mu^e)$ be

$$\begin{aligned} P(\lambda;\mu^e) &= \det\bigl(\lambda I_n - J(x^e,\mu^e)\bigr) \\ &= p_0(\mu^e)\lambda^n + p_1(\mu^e)\lambda^{n-1} + \cdots + p_n(\mu^e), \end{aligned} \tag{3}$$

where I_n is the n-dimensional identity matrix. The following matrix is introduced.

$$H_n(\mu^e) = \begin{bmatrix} p_1(\mu^e) & p_0(\mu^e) & \cdots & 0 \\ p_3(\mu^e) & p_2(\mu^e) & \cdots & 0 \\ \vdots & \vdots & \ddots & \vdots \\ p_{2n-1}(\mu^e) & p_{2n-2}(\mu^e) & \cdots & p_n(\mu^e) \end{bmatrix}, \tag{4}$$

where $p_i(\mu^e) = 0$ if $i < 0$ or $i > n$. Then, the conditions (i) and (ii) are respectively equivalent to the following conditions:

(i) Eigenvalue crossing condition:

$$\begin{aligned} &p_n(\mu^e) > 0, \\ &\Delta_i(\mu^e) = \det\bigl(H_i(\mu^e)\bigr) > 0, \quad i = 1,\ldots,n-2, \\ &\Delta_{n-1}(\mu^e) = \det\bigl(H_{n-1}(\mu^e)\bigr) = 0. \end{aligned} \tag{5}$$

(ii) Transversality condition:

$$\left.\frac{d(\Delta_{n-1}(\mu))}{d\mu}\right|_{\mu=\mu^e} \neq 0. \tag{6}$$

3. The proposed Hopf bifurcation control law

Suppose that, when μ is varied, the system (1) undergoes Hopf bifurcations at two points (x^{e1},μ^{e1}) and (x^{e2},μ^{e2}). The objective of Hopf bifurcation control here is to design a control law u such that both the Hopf bifurcation points (x^{e1},μ^{e1}) and (x^{e2},μ^{e2}) are relocated to new positions, say $(\bar{x}^{e1},\bar{\mu}^{e1})$ and $(\bar{x}^{e2},\bar{\mu}^{e2})$, respectively. A general dynamic state-feedback control law can be formulated as follows:

$$\begin{aligned} u &= u(x,y), \\ \dot{y} &= g(x,y), \end{aligned} \tag{7}$$

where $y \in R^m$ $(1 \leqslant m \leqslant n)$ is the state vector of the controller, and the feedback control $u(x,y)$ and the vector field $g(x,y)$ are smooth in x and y. Specifically, the following feedback control law having a linear term and a cubic term is proposed.

$$\begin{aligned} u_i(x_i,y_i) &= k_{1i}x_i + k_{3i}\bigl(x_i - \bar{x}_i^{e1}\bigr)^3 - l_i y_i, \\ \dot{y}_i &= u_i(x_i,y_i), \end{aligned} \tag{8}$$

where $\bar{x}_i^{e1}$ $(i = 1,2,\ldots,m)$ are the equilibrium values of x_i at the first designated Hopf bifurcation point, $K_1 = [k_{11},k_{12},\ldots,k_{1m}]$ and $K_3 = [k_{31},k_{32},\ldots,k_{3m}]$ are the control gain vectors, and $L = [l_1,l_2,\ldots,l_m]$ is the constant parameter vector.

Without lost of generality, we can assume that m control components u_i, $i = 1,2,\ldots,m$, are added to the first m equations of the system (1). Then, the closed-loop control system can be written as follows:

$$\begin{aligned} \dot{x} &= f(x,\mu) + u(x,y), \\ \dot{y} &= g(x,y), \end{aligned} \tag{9}$$

where $u(x,y) = [u_1(x_1,y_1),\ldots,u_m(x_m,y_m),0,\ldots,0]^T$ and $g(x,y) = [u_1(x_1,y_1),\ldots,u_m(x_m,y_m)]^T$. Owing to the incorporation of the controller, the dimension of the controlled system becomes $n+m$. It should be noted that, with the proposed control law in (8), the equilibria of the controlled system (9) are the ones of the original system (1) as well. Preserving the equilibria structure of the original system during the control process is one of the essential characteristics required in bifurcation control.

Remark 1. In some cases, the control objective can be achieved by using only one control component u_i. If more than one control components are used, some control gains k_{1i} or k_{3i} can be set to zero as long as the control input vector $u(x,y)$ still contains both the linear and the cubic terms.

Remark 2. It is well known that the cubic term occurring in a nonlinear system undergoing a Hopf bifurcation influences the stability of the bifurcated solutions [10]. Therefore, if the control objective is to relocate only one Hopf bifurcation point to a desired location, then the control gain vector K_3 can be used to control the stability of the created bifurcation solutions (see Example 2).

Remark 3. Let $z_i = k_{1i}x_i + k_{3i}(x_i - \bar{x}_i^{e1})^3$. Then, z_i (as a function of x_i) plays the role of input in the second equation of (8). In the Laplace domain, (8) yields the following.

$$\begin{aligned} u_i(s) &= -l_i y_i(s) + z_i(s), \\ (s+l_i)y_i(s) &= z_i(s). \end{aligned} \tag{10}$$

Then, the transfer function from the input z_i to the output u_i becomes

$$G_i(s) = \frac{u_i(s)}{z_i(s)} = \frac{s}{s+l_i}. \tag{11}$$

From (11), it can be seen that, all l_i must be positive to guarantee the stability of the control law in (8).

In what follows, we will show how to determine the control gain vectors K_1 and K_3 such that the controlled system (9) associated with the control law (8) undergoes Hopf bifurcations at $(\bar{x}^{e1},\bar{\mu}^{e1})$ and $(\bar{x}^{e2},\bar{\mu}^{e2})$. For the sake of convenience, we write the closed-loop control system (9) in the following form.

$$\dot{X} = F(X,\mu), \tag{12}$$

where $X = [x, y]^T$ and $F = [f(x,\mu) + u(x,y), g(x,y)]^T$. Letting $J_c(X,\mu) = \partial F(X,\mu)/\partial X$ be the Jacobian matrix of the closed-loop system (12), we can rewrite J_c as

$$J_c(X,\mu) = \begin{bmatrix} J(x) + A(X) & B(X) \\ C(X) & D(X) \end{bmatrix}, \tag{13}$$

where $J(x) = \partial f(x,\mu)/\partial x$, $A(X) = \partial u(x,y)/\partial x$, $B(X) = \partial u(x,y)/\partial y$, $C(X) = \partial g(x,y)/\partial x$, and $D(X) = \partial g(x,y)/\partial y$. The matrices $A(X)$, $B(X)$, $C(X)$ and $D(X)$ are given as follows.

$$A(X) = \begin{bmatrix} M & 0_{(n-m)\times(n-m)} \\ 0_{(n-m)\times(n-m)} & 0_{(n-m)\times(n-m)} \end{bmatrix},$$
$$B(X) = \begin{bmatrix} N \\ 0_{(n-m)\times m} \end{bmatrix},$$
$$C(X) = [\, M \quad 0_{m\times(n-m)} \,], \qquad D(X) = N, \tag{14}$$

where the matrices M and N are defined as

$$M = \operatorname{diag}\big(k_{11} + 3k_{31}(x_1 - \bar{x}_1^{e1})^2, \ldots, k_{1m} + 3k_{3m}(x_m - \bar{x}_m^{e1})^2\big),$$
$$N = \operatorname{diag}(-l_1, \ldots, -l_m). \tag{15}$$

3.1. K_1 determines the Hopf bifurcation at $(\bar{x}^{e1}, \bar{\mu}^{e1})$

At $\mu = \bar{\mu}^{e1}$, the equilibrium point of the controlled system (12) is $\bar{X}^{e1} = (\bar{x}^{e1}, \bar{y}^{e1})$, where $\bar{y}_i^{e1} = k_{1i}\bar{x}_i^{e1}/l_i$. Therefore, the matrix M in (15) becomes $M = \operatorname{diag}(k_{11}, \ldots, k_{1m})$. It is obvious that the Jacobian matrix $J_c(\bar{X}^{e1}, \bar{\mu}^{e1})$ does not depend on the control gain vector K_3. In other words, only the control gain vector K_1 contributes to the location of the Hopf bifurcation at $(\bar{x}^{e1}, \bar{\mu}^{e1})$. The characteristic polynomial of the Jacobian matrix $J_c(\bar{X}^{e1}, \bar{\mu}^{e1})$ is given by

$$P(\lambda; \bar{\mu}^{e1}) = p_0(\bar{\mu}^{e1})\lambda^{n+m} + p_1(\bar{\mu}^{e1})\lambda^{n+m-1} + \cdots + p_{n+m}(\bar{\mu}^{e1}). \tag{16}$$

Then, according to the conditions for the emergence of Hopf bifurcation (5) and (6), the control gain vector K_1 is obtained by solving the following equation.

$$\Delta_{n+m-1}(\bar{\mu}^{e1}) = \det\big(H_{n+m-1}(\bar{\mu}^{e1})\big) = 0, \tag{17}$$

under the constraints

$$p_{n+m}(\bar{\mu}^{e1}) > 0,$$
$$\Delta_i(\bar{\mu}^{e1}) = \det\big(H_i(\bar{\mu}^{e1})\big) > 0, \quad i = 1, \ldots, n+m-2,$$
$$\left.\frac{d(\Delta_{n+m-1}(\mu))}{d\mu}\right|_{\mu=\bar{\mu}^{e1}} \neq 0, \tag{18}$$

where the matrices $H_i(\bar{\mu}^{e1})$ $(i = 1, \ldots, n+m-2)$ are defined as in (4).

3.2. K_3 determines the Hopf bifurcation at $(\bar{x}^{e2}, \bar{\mu}^{e2})$

After determining the control gain vector $K_1 = K_1^*$, a Hopf bifurcation was created at the desired location $(\bar{x}^{e1}, \bar{\mu}^{e1})$ irrespective of the value of K_3. Next, we will deduce the control gain vector K_3 such that another Hopf bifurcation occurs at $(\bar{x}^{e2}, \bar{\mu}^{e2})$. At this point, the equilibrium point of the controlled system (12) is given by $\bar{X}^{e2} = (\bar{x}^{e2}, \bar{y}^{e2})$, where $\bar{y}_i^{e2} = [k_{1i}^*\bar{x}_i^{e2} + k_{3i}(\bar{x}_i^{e2} - \bar{x}_i^{e1})^3]/l_i$. The matrix M in (15) becomes

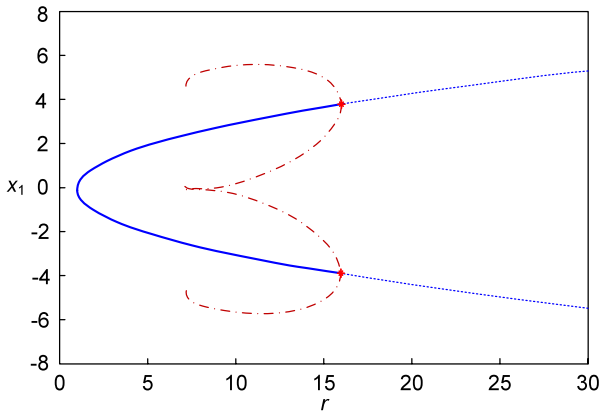

Fig. 1. Bifurcation diagram of the uncontrolled thermal convection loop model.

$$M = \operatorname{diag}\big(k_{11}^* + 3k_{31}(\bar{x}_1^{e2} - \bar{x}_1^{e1})^2, \ldots, k_{1m}^* + 3k_{3m}(\bar{x}_1^{e2} - \bar{x}_1^{e1})^2\big). \tag{19}$$

Then, we obtain the Jacobian matrix $J_c(\bar{X}^{e2}, \bar{\mu}^{e2})$ in the form of (13), that is dependent only on the control gain vector K_3. Finally, the control gain vector K_3 is obtained in the same way as that K_1 was obtained, see (16) to (18).

4. Numerical examples

4.1. Example 1

Consider a 3-D thermal convection loop model [17] described by

$$\dot{x}_1 = -4x_1 + 4x_2,$$
$$\dot{x}_2 = -x_1x_3 - x_2,$$
$$\dot{x}_3 = x_1x_2 - x_3 - r \tag{20}$$

where $r \in R$ is the bifurcation parameter. Without control, the system (20) undergoes Hopf bifurcations at two points $(x_1^{e1}, x_2^{e1}, x_3^{e1}) = (3.87298, 3.87298, -1)$ and $(x_1^{e2}, x_2^{e2}, x_3^{e2}) = (-3.87298, -3.87298, -1)$ corresponding to the values of the bifurcation parameter as $r^{e1} = r^{e2} = 16$, as shown in Fig. 1. Here, the thick solid lines represent stable equilibrium points, while the dotted line represents unstable ones. The maxima and minima of unstable limit cycles are indicated by dashed lines. Note that all the bifurcation diagrams in this Letter were produced using the XPPAUT software package [22]. Assume that only the control component $u_1(x_1, y_1)$ is added to the right-hand side of the first equation of (20). In vector form, the controlled system is given by

$$\dot{X} = F(X, r), \tag{21}$$

where $X = [x_1, x_2, x_3, y_1]^T$ and

$$F(X,r) = \begin{bmatrix} -4x_1 + 4x_2 + u_1(x_1, y_1) \\ -x_1x_3 - x_2 \\ x_1x_2 - x_3 - r \\ u_1(x_1, y_1) \end{bmatrix} = \begin{bmatrix} -4x_1 + 4x_2 + k_{11}x_1 + k_{31}(x_1 - \bar{x}_1^{e1})^3 - l_1y_1 \\ -x_1x_3 - x_2 \\ x_1x_2 - x_3 - r \\ k_{11}x_1 + k_{31}(x_1 - \bar{x}_1^{e1})^3 - l_1y_1 \end{bmatrix}. \tag{22}$$

Here, we set $l_1 = 0.5$. The control objective is to advance the upper Hopf bifurcation point toward to $\bar{r}^{e1} = 10$, and move the lower Hopf bifurcation point to $\bar{r}^{e2} = 20$.

(a) *Determination of control gain* k_{11}

At $\bar{r}^{e1} = 10$, the upper equilibrium point of the controlled system (21) is $\bar{X}^{e1} = (\bar{x}_1^{e1}, \bar{x}_2^{e1}, \bar{x}_3^{e1}, \bar{y}_1^{e1}) = (3, 3, -1, 2k_{11})$. Therefore, we have

$$J(\bar{x}^{e1}) = \begin{bmatrix} -4 & 4 & 0 \\ 1 & -1 & -3 \\ 3 & 3 & -1 \end{bmatrix}, \qquad A(\bar{X}^{e1}) = \begin{bmatrix} k_{11} & 0 & 0 \\ 0 & 0 & 0 \\ 0 & 0 & 0 \end{bmatrix},$$
$$B(\bar{X}^{e1}) = \begin{bmatrix} -0.5 \\ 0 \\ 0 \end{bmatrix}, \qquad C(\bar{X}^{e1}) = [\, k_{11} \quad 0 \quad 0 \,],$$
$$D(\bar{X}^{e1}) = [-0.5]. \tag{23}$$

Using (13), the Jacobian matrix of (21) at $\bar{r}^{e1} = 10$ is obtained as follows.

$$J_c(\bar{X}^{e1}, \bar{r}^{e1}) = \begin{bmatrix} -4 + k_{11} & 4 & 0 & -0.5 \\ 1 & -1 & -3 & 0 \\ 3 & 3 & -1 & 0 \\ k_{11} & 0 & 0 & -0.5 \end{bmatrix}. \tag{24}$$

Then, the characteristic polynomial of $J_c(\bar{X}^{e1}, \bar{r}^{e1})$ is given by

$$P(\lambda; \bar{r}^{e1}) = p_0(\bar{r}^{e1})\lambda^4 + p_1(\bar{r}^{e1})\lambda^3 + p_2(\bar{r}^{e1})\lambda^2 + p_3(\bar{r}^{e1})\lambda + p_4(\bar{r}^{e1}), \tag{25}$$

where $p_0(\bar{r}^{e1}) = 1$, $p_1(\bar{r}^{e1}) = 6.5 - k_{11}$, $p_2(\bar{r}^{e1}) = 17 - 2k_{11}$, $p_3(\bar{r}^{e1}) = 79 - 10k_{11}$, $p_4(\bar{r}^{e1}) = 36$. Subject to the conditions in (17) and (18), we obtain the value of k_{11} as $k_{11} = k_{11}^* = 0.82303$.

(b) *Determination of control gain* k_{31}

At $\bar{r}^{e2} = 20$, the lower equilibrium point of the controlled system (21) becomes $\bar{X}^{e2} = (\bar{x}_1^{e2}, \bar{x}_2^{e2}, \bar{x}_3^{e2}, \bar{y}_1^{e2}) = (-4.35890, -4.35890, -1, 1.64606 + 797.01870k_{31})$. Then, the following are obtained.

$$J(\bar{x}^{e2}) = \begin{bmatrix} -4 & 4 & 0 \\ 1 & -1 & 4.35890 \\ -4.35890 & -4.35890 & -1 \end{bmatrix},$$
$$A(\bar{X}^{e2}) = \begin{bmatrix} 0.82303 + 162.46018k_{31} & 0 & 0 \\ 0 & 0 & 0 \\ 0 & 0 & 0 \end{bmatrix},$$
$$B(\bar{X}^{e2}) = \begin{bmatrix} -0.5 \\ 0 \\ 0 \end{bmatrix},$$
$$C(\bar{X}^{e2}) = [\, 0.82303 + 162.46018k_{31} \quad 0 \quad 0 \,],$$
$$D(\bar{X}^{e2}) = [-0.5]. \tag{26}$$

Using (13), we obtain the Jacobian matrix of (21) at $\bar{r}^{e2} = 20$ as follows.

$$J_c(\bar{X}^{e2}, \bar{r}^{e2}) = \begin{bmatrix} -3.17697 + 162.46018k_{31} & 4 & 0 & -0.5 \\ 1 & -1 & 4.35890 & 0 \\ -4.35890 & -4.35890 & -1 & 0 \\ 0.82303 + 162.46018k_{31} & 0 & 0 & -0.5 \end{bmatrix}. \tag{27}$$

The characteristic polynomial of $J_c(\bar{X}^{e2}, \bar{r}^{e2})$ is then given by

$$P(\lambda; \bar{r}^{e2}) = p_0(\bar{r}^{e2})\lambda^4 + p_1(\bar{r}^{e2})\lambda^3 + p_2(\bar{r}^{e2})\lambda^2 + p_3(\bar{r}^{e2})\lambda + p_4(\bar{r}^{e2}), \tag{28}$$

where $p_0(\bar{r}^{e2}) = 1$, $p_1(\bar{r}^{e2}) = 5.67697 - 162.46020k_{31}$, $p_2(\bar{r}^{e2}) = 25.35393 - 324.92036k_{31}$, $p_3(\bar{r}^{e2}) = 147.53935 - 3249.20360k_{31}$, and $p_4(\bar{r}^{e2}) = 76$. By solving (17) and (18) with respect to k_{31}, we obtain $k_{31} = k_{31}^* = -0.00794$.

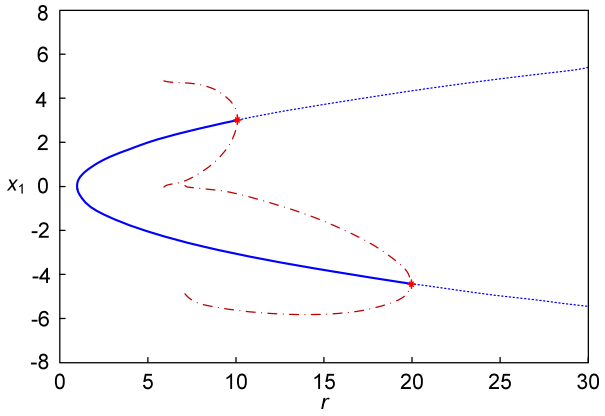

Fig. 2. Bifurcation diagram of the controlled thermal convection loop model with $k_{11} = 0.82303$ and $k_{31} = -0.00794$.

The bifurcation diagram of the controlled system is shown in Fig. 2. As expected, the upper and the lower Hopf bifurcation points have been successfully relocated to new positions at $\bar{r}^{e1} = 10$ and $\bar{r}^{e2} = 20$, respectively.

4.2. Example 2

We have shown in Example 1 that the proposed control law in (8) is capable of relocating two Hopf bifurcation points in a nonlinear system to any designated locations. Here, we will show that when the control objective is to relocate only one Hopf bifurcation point, the stability of the created bifurcation solution can be controlled as well by using the proposed control law in (8). Let us consider a 4-D Hodgkin–Huxley neuron model [23] described by

$$\begin{aligned} \dot{x}_1 &= I - 36x_2^4(x_1 + 12) - 120x_3^3x_4(x_1 - 120) - 0.3(x_1 - 10.6), \\ \dot{x}_2 &= \alpha_2(x_1)(1 - x_2) - \beta_2(x_1)x_2, \\ \dot{x}_3 &= \alpha_3(x_1)(1 - x_3) - \beta_3(x_1)x_3, \\ \dot{x}_4 &= \alpha_4(x_1)(1 - x_4) - \beta_4(x_1)x_4, \end{aligned} \tag{29}$$

where I represents the external applied current, which is considered as a bifurcation parameter. The parameters α_2, β_2, α_3, β_3, α_4 and β_4 are functions of x_1 as follows [23]:

$$\begin{aligned} \alpha_2(x_1) &= 0.01(10 - x_1)/\{\exp[(10 - x_1)/10] - 1\}, \\ \beta_2(x_1) &= 0.125\exp(-x_1/80), \\ \alpha_3(x_1) &= 0.1(25 - x_1)/\{\exp[(25 - x_1)/10] - 1\}, \\ \beta_3(x_1) &= 4.0\exp(-x_1/18), \\ \alpha_4(x_1) &= 0.07\exp(-x_1/20), \\ \beta_4(x_1) &= 1/\{\exp[(30 - x_1)/10] + 1\}. \end{aligned} \tag{30}$$

Without control, the bifurcation diagram of x_1 as a function of I is shown in Fig. 3. Here, the thick solid lines represent stable equilibrium points, while the dotted line represents unstable ones. The maxima and minima of stable and unstable limit cycles are indicated by thin and dashed lines, respectively. From Fig. 3, it can be seen that the Hodgkin–Huxley model undergoes Hopf bifurcations at two critical values in the external applied current I. The left Hopf bifurcation point occurs at $I^{e1} = 8.4103$ and the right Hopf bifurcation point occurs at $I^{e2} = 163.3474$. It can also be seen that the left Hopf bifurcation is subcritical (i.e., the bifurcated limit cycle is unstable).

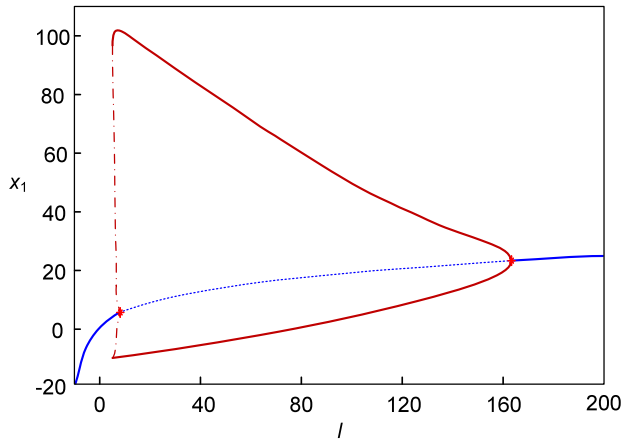

Fig. 3. Bifurcation diagram of the uncontrolled Hodgkin–Huxley neuron model.

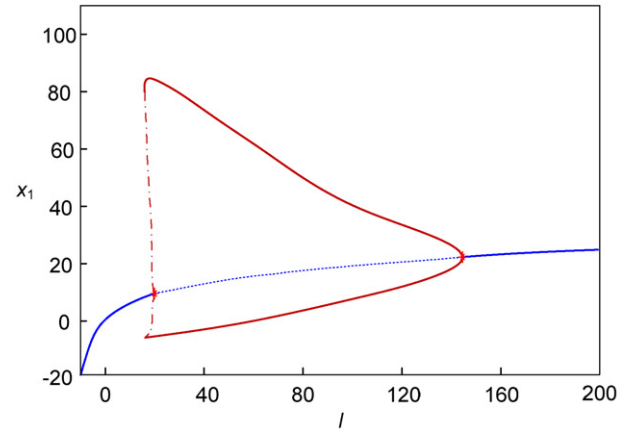

Fig. 4. Bifurcation diagram of the controlled Hodgkin–Huxley neuron model with $k_{11} = -0.68870$ and $k_{31} = 0$.

The goals of control here are (i) to move the left Hopf bifurcation point to $\bar{I}^{e1} = 20$ and (ii) to stabilize the created Hopf bifurcation solution. We select only the state variable x_1 to be controlled. Therefore, the control law can be described as follows.

$$u_1(x_1, y_1) = k_{11}x_1 + k_{31}\left(x_1 - \bar{x}_1^{e1}\right)^3 - l_1 y_1,$$
$$\dot{y}_1 = k_{11}x_1 + k_{31}\left(x_1 - \bar{x}_1^{e1}\right)^3 - l_1 y_1, \tag{31}$$

where $\bar{x}_1^{e1} = 8.51830$ is the equilibrium value of x_1 at $\bar{I}^{e1} = 20$. As explained in Section 3.1 (also in Example 1), the conditions for the occurrence of a Hopf bifurcation at $\bar{I}^{e1} = 20$ can be satisfied through control gain k_{11}. The equilibrium point of the controlled Hodgkin–Huxley neuron model at $\bar{I}^{e1} = 20$ is obtained as $\bar{X}^{e1} = (\bar{x}_1^{e1}, \bar{x}_2^{e1}, \bar{x}_3^{e1}, \bar{x}_4^{e1}, \bar{y}_1^{e1}) = (8.51830, 0.45223, 0.13612, 0.30436, 17.0366k_{11})$. Here, we set $l_1 = 0.1$. Then, following the procedure in Section 3.1, we obtain the value of k_{11} as $k_{11} = k_{11}^* = -0.68870$. Since k_{31} has no effect on the location of the created Hopf bifurcation point, we temporarily set $k_{31} = 0$, and calculate the bifurcation diagram of the controlled system, as shown in Fig. 4. As expected, the left Hopf bifurcation point has been successfully shifted to $\bar{I}^{e1} = 20$, and it is still subcritical.

Next, we will show that by choosing a proper value of control gain k_{31}, the stability of the created bifurcation solution can be achieved. Fig. 5 shows the bifurcation diagram of the controlled Hodgkin–Huxley with $k_{11} = -0.68870$ and $k_{31} = -0.0075$. Obviously, the bifurcated limit cycle is stable or the created Hopf bifurcation is supercritical. Note that in order to derive the analytical expression of the stability condition for the created bifurcation solution with respect to k_{31}, one may employ the center manifold theory and normal form reduction as presented in [18].

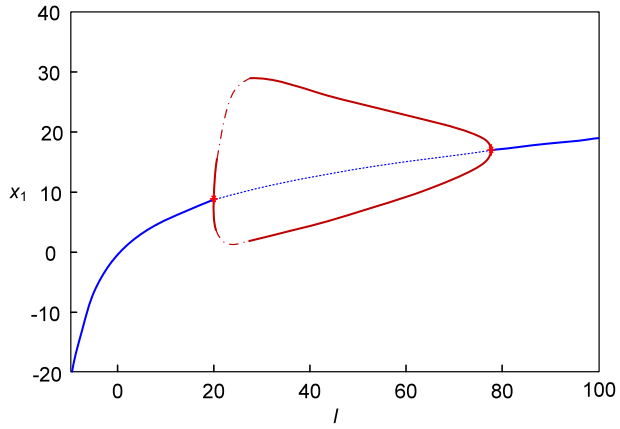

Fig. 5. Bifurcation diagram of the controlled Hodgkin–Huxley neuron model with $k_{11} = -0.68870$ and $k_{31} = -0.0075$.

5. Conclusions

In this Letter, we addressed the problem of controlling Hopf bifurcations in nonlinear systems. We proposed a novel dynamic state-feedback control law capable of relocating two Hopf bifurcation points to any desired locations simultaneously. We also derived analytically the procedure to determine the control gains. The effectiveness of the proposed control method was verified through numerical examples.

Acknowledgement

This research was supported by the World Class University program through the National Research Foundation of Korea funded by the Ministry of Education, Science and Technology, Republic of Korea (grant No. R31-20004).

References

[1] H.O. Wang, E.H. Abed, A.M.A. Hamdan, IEEE Trans. Circuits Systems I Fund. Theory Appl. 41 (1994) 294.
[2] A.M. Harb, N. Abdel-Jabbar, Chaos Solitons Fractals 18 (2003) 1055.
[3] D.C. Liaw, E.H. Abed, Automatica 32 (1) (1996) 109.
[4] M.A. Nayfed, E.H. Abed, Automatica 38 (2002) 995.
[5] H.O. Wang, D. Chen, G. Chen, Bifurcation control of pathological heart rhythms, in: Proceedings of the IEEE Conference on Control Applications, Trieste, Italy, 1–4 September, 1997, pp. 858–862.
[6] Y. Xie, L. Chen, Y.M. Kang, K. Aihara, Phys. Rev. E 77 (2008) 061921.
[7] Y. Xie, K. Aihara, Y.M. Kang, Phys. Rev. E 77 (2008) 021917.
[8] M.A. Kramer, B.A. Lopour, H.E. Kirsch, A.J. Szeri, Phys. Rev. E 73 (2006) 041928.
[9] G. Chen, J.L. Moiola, H.O. Wang, Int. J. Bifur. Chaos 10 (3) (2000) 511.
[10] E.H. Abed, J.H. Fu, Systems Control Lett. 7 (1986) 11.
[11] H.O. Wang, E.H. Abed, Automatica 31 (9) (1995) 1213.
[12] A. Tesi, E.H. Abed, R. Genesio, H.O. Wang, Automatica 32 (9) (1996) 1255.
[13] P. Yu, G. Chen, Int. J. Bifur. Chaos 14 (5) (2004) 1683.
[14] L.F. Mello, S.F. Coelho, Phys. Lett. A 373 (2009) 1116.
[15] D. Wei, X. Luo, Y. Qin, Nonlinear Dyn. 63 (2011) 323.
[16] N. Vasegh, A.K. Sedigh, Phys. Lett. A 372 (2008) 5110.
[17] D.S. Chen, H.O. Wang, G. Chen, IEEE Trans. Circuits Systems I Fund. Theory Appl. 48 (6) (2001) 661.
[18] G. Wen, D. Xu, Phys. Lett. A 337 (2005) 93.
[19] S. Zhou, X. Liao, J. Yu, K.W. Wong, Phys. Lett. A 338 (2005) 261.
[20] M. Luo, Y. Wu, J. Peng, Biol. Cybern. 101 (2009) 241.
[21] W.M. Liu, J. Math. Anal. Appl. 182 (1994) 250.
[22] B. Ermentrout, Simulating, Analyzing, and Animating Dynamical Systems: A Guide to XPPAUT for Researchers and Students, SIAM, Philadelphia, 2002.
[23] E.M. Izhikevich, Dynamical Systems in Neuroscience: The Geometry of Excitability and Bursting, The MIT Press, England, 2007.